



Surfactant-dependent photoluminescence of CdTe/CdS nanocrystals

Karolis Virzbickas, Laura Rimkute, Andrew J Harvie & Kevin Critchley

To cite this article: Karolis Virzbickas, Laura Rimkute, Andrew J Harvie & Kevin Critchley (2017) Surfactant-dependent photoluminescence of CdTe/CdS nanocrystals, Journal of Experimental Nanoscience, 12:1, 94-103, DOI: [10.1080/17458080.2016.1273553](https://doi.org/10.1080/17458080.2016.1273553)

To link to this article: <http://dx.doi.org/10.1080/17458080.2016.1273553>



© 2017 The Author(s). Published by Informa UK Limited, trading as Taylor & Francis Group



Published online: 31 Jan 2017.



Submit your article to this journal [↗](#)



Article views: 182



View related articles [↗](#)



View Crossmark data [↗](#)

Surfactant-dependent photoluminescence of CdTe/CdS nanocrystals

Karolis Virzbickas, Laura Rimkute, Andrew J Harvie and Kevin Critchley

School of Physics and Astronomy, University of Leeds, Leeds, LS2 9JT, UK

ABSTRACT

The photoluminescence of aqueously synthesised core/shell CdTe/CdS quantum dots (QDs) was investigated. Two molar ratios (2.4 and 1.3) of thioglycolic acid (TGA) to Cd^{2+} were compared to determine the best synthesis conditions for high photoluminescent quantum yield (PLQY) and photostability. A difference in the PLQY of the CdTe/CdS QDs was observed when CdS shells were grown with different TGA/ Cd^{2+} ratios. The difference in the observed PLQY was attributed to the quality of the passivation of the CdTe during the CdS shell growth. At TGA/ Cd^{2+} ratio of 1.3, the CdS shell forms through homogeneous nucleation, which is limited by diffusion of growth material from the solution onto the QDs surface. Due to the lattice mismatch of CdTe and CdS, the core will experience coherence strain resulting in dislocation sites and surface defects between nucleation sites which can result in non-radiative trap states. When the TGA/ Cd^{2+} ratio is 2.0, the CdS shell grows epitaxially, minimising the number of surface trap states. Finally, we observed that the fluorescence intermittency was suppressed for CdTe QDs after UV light illumination, attributed to annealing of deep surface trap states by UV light.

ARTICLE HISTORY

Received 24 August 2016
Accepted 9 December 2016

KEYWORDS

CdTe/CdS;
photoluminescence; TGA;
blinking; photostability

1. Introduction

Colloidal quantum dots (QDs) have attracted a lot of attention over the past few decades due to their size-dependent properties [1,2]. Their brightness [3], photostability [4], surface functionality and size-tunable emission [5] set them apart from other fluorescent materials such as organic dyes. The physical properties can be tuned to meet specific requirements by changing the chemical composition [6,7], particle size and shape [8], surface chemistry and interfacial structures [9]. QDs can be synthesised using either organic [10] or aqueous [1,11] methods. The aqueous methods are considered to be simpler, cheaper and less toxic to environment [12] with the ability to produce highly luminescent [13], surface functionalised [14] and biocompatible [15] QDs. Low photoluminescence quantum yield (PLQY) from QDs is often observed due to surface trap states [16,17]. A number of strategies are employed to increase PLQY by reducing the surface trap state

CONTACT Kevin Critchley  k.critchley@leeds.ac.uk

The data associated with this paper are openly available from the University of Leeds data repository, doi:  <http://doi.org/10.5518/144>

density. For example, highly photoluminescent CdTe QDs were synthesised hydrothermally [18,19] at 180 °C to achieve crystalline, monodisperse QDs with apparent low densities of surface trap states. In another study, microwave irradiation was used to achieve very highly luminescent CdTe QDs (by dielectric heating) [20,21]. Additional methods include variation of the precursor concentration [19,22,23] and altering the pH of the QDs solution [22,23].

A common strategy used to improve the spectral properties of QDs involves the growth of a ‘shell’ of a wide-band-gap semiconductor around the QD ‘core’. The growth of shells onto CdTe cores passivates the ‘dangling bonds’, which form trap states, reducing the frequency of non-radiative recombination events. The addition of the shell can have the effect of enhancing the chemical and photostability of the QDs, whilst maintaining confinement of the holes, electrons or both holes and electrons [24]. For good surface passivation, the shell and core materials should have closely matching lattice constants; eg CdTe and CdS crystals have lattice constants of 6.482 and 6.714 Å [25], respectively, a mismatch of 3.45%. This lattice mismatch between the shell and the core induces a coherence strain which can result in the formation of defect states at the core/shell interface [26]. Coherence strain acts on the CdS shell, which causes the shell material to adapt to the core lattice parameters. With increasing CdS shell thickness, dislocations are formed to relieve the coherence strain and keep partial lattice parameter match. These defect sites act as trap states for photogenerated charge carriers, which decrease the PLQY of the QDs via increase in non-radiative recombination. It has been reported that the growth of approximately two CdS monolayers can produce the highest PLQY [26].

Interestingly, forming CdS complexes at the surface of the CdTe QDs cores using illumination has also been shown to increase the PLQY [27]. Using thioglycolic acid (TGA) as a surfactant during CdTe growth creates a sulphur rich surface environment, similar to when a CdS shell is grown on CdTe cores QDs as a two-stage process [27]. Upon UV light illumination of TGA stabilised CdTe QDs, free sulphur ions are produced through photocatalytic oxidation of TGA [28]. Free sulphur ions react with the Cd²⁺ on the QD core surfaces to form CdS. Therefore, with continuous UV radiation a full CdS shell can be grown on the core CdTe QDs. If there is an excess of TGA surfactant and Cd²⁺ ions in the solution, then a CdS shell can be grown during continuous UV light illumination. Recently, it was shown that UV light ($\lambda = 365$ nm) could be used to grow CdS shell on CdTe core QDs by TGA photolysis [29].

Furthermore, optimisation of the TGA/Cd²⁺ ratio yields high PLQY (65%) CdTe QDs [12,19,30]. It was found that decreasing the proportion of TGA to Cd²⁺ increases the relative concentration of Cd-thiol complexes in the solution and yields QDs with better surface passivation [23]. In addition, the ratio must be high enough in order to passivate the surface of QDs and provide colloidal stability in aqueous environment. At an optimum TGA/Cd²⁺ ratio, the QDs are provided with the most complete surface passivation by sulphur ions while still being stable in aqueous environment [12]. At higher TGA/Cd²⁺ ratios where QDs surface is covered with the excess amount of surfactant molecules, the TGA cannot attach to the surface effectively thereby creating some non-radiative defect centres [23,30]. The type of surfactants, chemical structure and condition of synthesis affect the reactivity of QDs surface and thus control the growth of QDs leading to a variation in the PLQY values [31].

2. Experimental section

2.1. Materials

All chemicals studied were of analytical grade. Cadmium perchlorate hydrate (99%), TGA ($\geq 99\%$), sodium hydroxide ($\geq 98\%$), thiourea ($\geq 99\%$), sulphuric acid (99.999%), methanol (99.8%) and Rhodamine 6G were purchased from Sigma-Aldrich. Aluminium telluride pieces were purchased from CERAC and stored under N_2 . All materials were used as received.

2.2. Synthesis of core quantum dots

Core CdTe QD dispersions were prepared according to a previously reported method [1]. Typically, 1.095 g of $Cd(ClO_4)_2 \cdot 6H_2O$ was dissolved in 200 mL of Milli-Q water, and TGA was added at molar ratios of 1.3 and 2.4 with respect to Cd^{2+} . The pH of the solution was adjusted to 11.4 by drop-wise addition of a 1 M NaOH solution. The solution was deoxygenated by bubbling N_2 , through the solution. H_2Te gas was passed through the Cd^{2+} solutions by adding 15 mL of 0.5 M sulphuric acid to ~ 0.2 g of Al_2Te_3 in a three-neck flask. Clusters of CdTe were formed quickly after the introduction of H_2Te . CdTe nanocrystals grew by refluxing at $100^\circ C$. The molar ratios of 1.3 and 2.4 are referred to as high quantum yield (HQY) and low quantum yield (LQY), respectively.

2.3. Synthesis of core-shell quantum dots

The CdS shell was grown on the QDs core using two methods, represented here as methods A and B. In method A, 50 mg of thiourea powder was added to CdTe core QDs dispersion (50 mL) while the mixture was stirred under reflux at $100^\circ C$. The solution was refluxed for one hour and then left to cool to room temperature. In method B, a solution 10 mL containing thiourea (0.12 mmol), cadmium perchlorate (0.17 mmol) and TGA (0.16 mmol) was added to 10 mL of the CdTe cores before heating the solution. Thiourea is a source of sulphur for the shell growth in both methods. These quantities are consistent with the material needed to form approximately two monolayers of CdS on the surface of the CdTe cores. CdS shells were grown using both methods A and B on the HQY CdTe QDs, but only method A with LQY CdTe QDs. No further purification processes were used after the synthesis.

2.4. Experimental set-up

The UV-Vis absorption spectra were recorded with a Perkin-Elmer Model Lambda35 spectrophotometer. Photoluminescence (PL) spectra were recorded with a Perkin-Elmer Model LS55 spectrometer, using excitation wavelengths of 400 nm and 450 nm for QDs and Rhodamine 6G respectively. Photoluminescence Quantum Yield (PLQY) value was taken as 0.91 [32] for Rhodamine 6G dissolved in methanol. PLQY of CdTe QDs was calculated according to the method described in [33]. All measurements were taken of samples with optical density below 0.2 at excitation wavelengths. PL intensity stability was recorded at 60-s time interval after the sample was illuminated with UV light (375 nm) at 5-min time periods. Blinking experiment data were collected using an in-house built total

internal reflection fluorescence (TIRF) Nikon Eclipse TE300 microscope by exciting QDs at wavelength set to 410 nm and recording at 101 Hz. For the measurement, QDs were dried on the microscope slide under nitrogen flow. To investigate photostability, diluted solution of QDs was illuminated with 6W UV lamp where 95% of energy was emitted at 369 nm wavelength.

3. Results

3.1. Core and core-shell quantum dots

The core CdTe QDs were synthesised using a precursor ratio of 1:1.3 and 1:2.4 of Cd²⁺:TGA which will be here-on referred to as HQY and LQY (see section entitled: “Synthesis of core-shell quantum dots”). Fluorescence peak full widths at half maxima were 0.19 and 0.21 eV, which indicate monodisperse QDs. CdTe/CdS QDs were produced using methods A and B from CdTe QDs. The Stokes shifts, measured from excitation to PL peak maxima wavelength, for CdTe/CdS methods A and B were 41 and 45 nm, respectively. LQY CdTe/CdS QDs were synthesised only by method A, which resulted in Stokes shift of 42 nm.

3.2. Photostability of the core quantum dots

Figure 1 shows that HQY QDs exposed to UV light initially show a small increase in PL intensity before tending to decrease towards zero. For LQY QDs, a dramatic increase in PL intensity was observed after 5–10 min of UV illumination. This remained stable for ~10 min before the intensity decayed towards zero. The rate of the decay is lower for the HQY than for the LQY CdTe QDs. For both HQY and LQY QDs, PL increased after some time of UV light illumination and decreased to low values. Similar results were shown in previous studies [5,11,34]. The PL maximum wavelength did not shift during illumination. Illumination time periods represent the duration of time QDs were exposed to UV light. After each illumination, the PL was measured followed by further illumination.

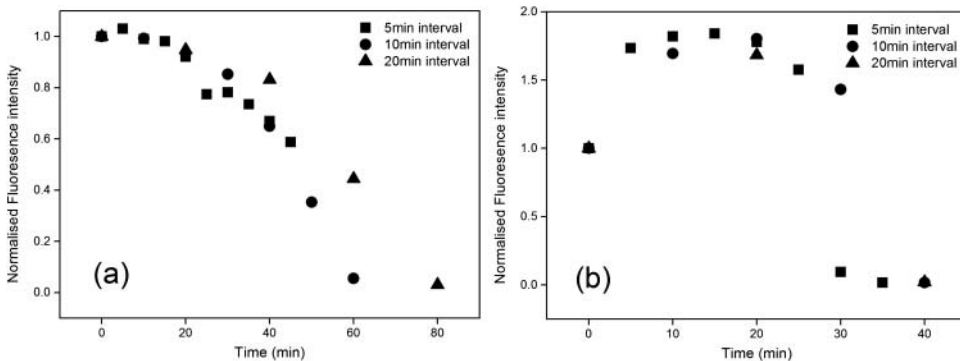


Figure 1. The normalised photoluminescence intensity plots of HQY (a) and LQY (b) QDs with increasing time of UV light illumination. Photoluminescence intensity was recorded at 5 min (square), 10 min (circle) and 20 min (triangle) time intervals of UV light (375 nm) illumination.

Figure 2 shows PLQY values of HQY and LQY CdTe QDs before and after growth of the CdS shell. Core HQY CdTe QDs had room temperature PLQY of $65\% \pm 2\%$ and after growing CdS shell with methods A and B the PLQY values were $51\% \pm 4\%$ and $41\% \pm 2\%$, respectively. This corresponds to $\sim 15\%$ and $\sim 24\%$ drop in PLQY value, respectively. However, LQY CdTe QDs displayed PLQY of $11.9\% \pm 0.5\%$ which increased to $19.9\% \pm 0.6\%$ after shell growth. These contrasting results are unexpected because by growing shell QDs optical properties are usually increased. In the case of HQY CdTe QDs CdS shell increased and for LQY CdTe QDs shell decreased the number of non-radiative defect sites.

3.3. Photoluminescence intensity stability

Figure 3(a) shows that the HQY QDs PL intensity was not stable after illumination. In most cases, the PL partially increased with time until reaching a plateau. In contrast, Figure 3(b) shows that the PL intensity of the LQY QDs does not increase with time. The PL intensity remains stable after the UV light illumination.

3.4. Blinking of the core quantum dots

The measurements of photoluminescence intensity vs time shown in figure for HQY CdTe QDs demonstrated that QDs intermittence on and off periods off 100 ms periods. The intensity was measured for a single CdTe QD with frequency of 100 Hz. The fluorescence intermittency (blinking) is typical for CdTe core nanocrystals. However, after 5 min of UV exposure, the CdTe QDs showed reduced 'off' periods during observation. PL images in Figure 4(b) show that the HQY CdTe QDs had fluorescence intermittency. For HQY CdTe QDs after 5 min of UV exposure the PL is more stable.

4. Discussion

4.1. Growth of CdS shell on CdTe core quantum dots

The PL increase shown after illumination (Figure 1) is attributed to reorganisation and annealing of the surface defect sites and unpassivated atoms, which act as traps for the

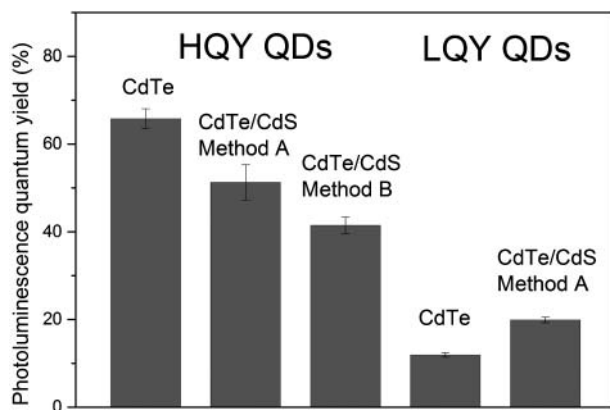


Figure 2. PLQY values of HQY and LQY CdTe QDs before and after growth of CdS shell.

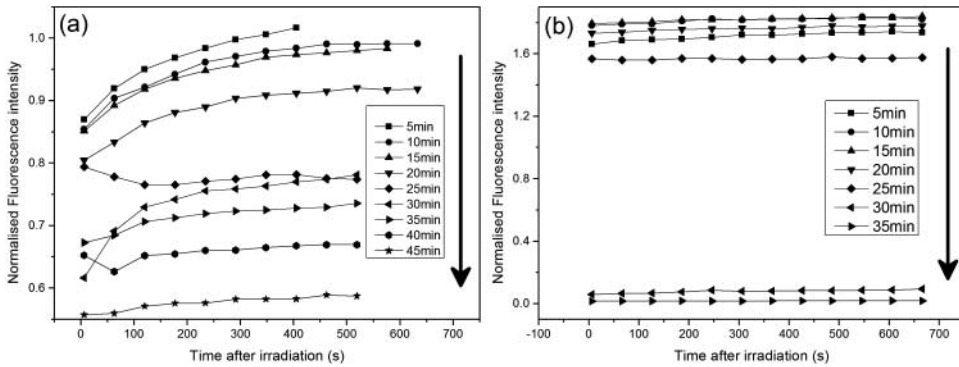


Figure 3. Normalised photoluminescence intensity with time plots after UV light illumination of HQY (a) and LQY (b) QDs.

photogenerated carriers. In particular, unpassivated Te^{2-} bonds are known to act as surface trap states for holes [11]. PL intensity decrease after an initial increase in Figure 1 can be explained by photo-oxidation of the surface ligands [28]. Photogenerated holes photo-oxidise surface ligands and leave non-radiative site on the surface, which quenches the PL [35]. The increase of PL should be more noticeable for the QDs with a higher number of surface defects which is seen in Figure 1(b). Thus, we conclude that PL behaviour during the UV light illumination for HQY and LQY QDs is attributed to the difference in the surface quality, which originates from the different growth conditions of CdTe QDs [5].

Results displayed in Figure 2 illustrate the CdS shell growth effect on HQY and LQY CdTe core QDs. During CdS shell addition, total growth is suppressed as the shell

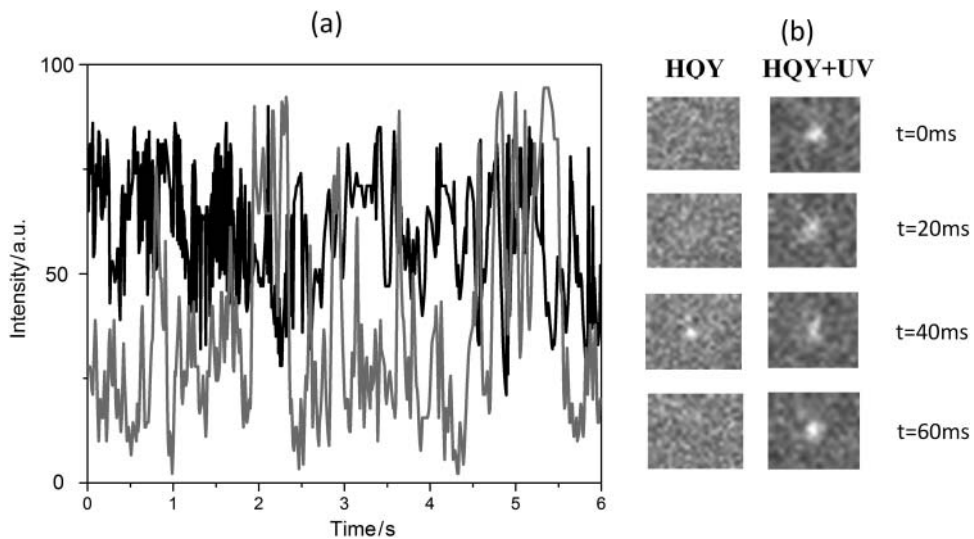


Figure 4. (Colour online). The TIRF photoluminescence intensity histogram for single HQY CdTe QDs (grey) and HQY CdTe QDs (black) after 5 min UV light illumination recorded at 100 Hz (a). The TIRF images of a single HQY CdTe QD before and after 5 min UV light illumination made at 20 ms intervals (b).

precursors compete with surfactant molecules for the CdTe QDs surface area. This will result in homogeneous nucleation of CdS shell under diffusion control of Cd and S materials. This would be a preferable condition for growth of CdTe core QDs, because it would provide QDs with best surface quality [5,12,36]. However, this can be undesirable because the CdS shell will experience coherence strain, which will result in the dislocation of sites and surface defects between nucleation sites where carriers charge can migrate and be trapped [26]. As a result, CdS shell synthesised by methods A and B with TGA/Cd²⁺ ratio set to 1.3 on HQY CdTe QDs introduced non-radiative sites and lowered PLQY. This was more prominent for method B because additional sulphur increased the number of nucleation sites. However, when the LQY CdTe/CdS shell was grown with TGA/Cd²⁺ ratio set to 2.4, TGA passivates the surface less efficiently, therefore providing smaller energy barrier to CdS shell growth. In these conditions, the CdS shell grows onto the LQY CdTe QDs epitaxially and the shell passivates the core without introducing additional trap states. This is further evident in Figure 5 where CdTe/CdS QDs Stokes shift can be seen. CdTe/CdS QDs with higher Stokes shifts is often indicative of increased densities of surface trap states. Method B produced the highest Stokes shift (Figure 5) with largest drop in PLQY.

This effect is further demonstrated in Figure 1 where PL intensity changes with time after UV light illumination for HQY CdTe QDs, but not for the LQY CdTe QDs. During UV light illumination, the QD surface reorganised leaving new unpassivated bonds, which quenches the PL. The PL intensity returns to stable position when free bonds are passivated by excess TGA molecule on the QDs surface or hydroxy ions in solution. In the case of HQY CdTe QDs, the time scale for bond passivation on the surface is longer because material transfer is governed by diffusion to the HQY CdTe QDs surface. These longer time scales can be seen in Figure 4(a) where PL intensity change with time can be seen. In the case of LQY CdTe QDs, TGA is in excess on the surface, which results in fast passivation of free bonds resulting in stable PL after illumination.

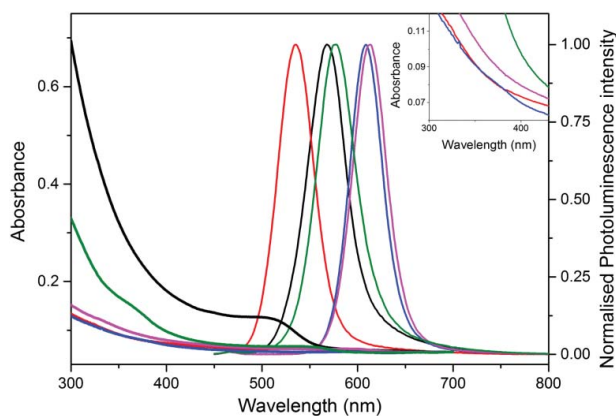


Figure 5. (Colour online). UV-Vis absorbance and photoluminescence spectra (excitation at 400 nm) of LQY (red), HQY (black) CdTe QDs and LQY CdTe/CdS method A (green), HQY CdTe/CdS method A (blue) and HQY CdTe/CdS method B (purple).

4.2. TGA ratio and CdS shell effect on the optical properties of quantum dots

This blinking is governed by non-radiative Auger recombination [37] and is dependent mostly on the surface properties of QDs [38–40]. Any change in blinking is considered a result of a surface change. CdTe/CdS core/shell systems were shown to suppress blinking, but only with thicker shells where the electron and hole are segregated, respectively, to the shell and core [41,42]. However, the observed red shift was too small to indicate formation of CdS shell on CdTe core, and thus blinking behaviour cannot be explained by charge separation.

Although there are other explanations for blinking, the literature suggests that the primary mechanism can be explained by a model where a photogenerated hole is trapped in a deep surface trap via a non-radiative relaxation process, governed by the Auger mechanism [43]. This explains the blinking differences between HQY QDs and same QDs after exposure to UV light in Figure 4. Initially, core QDs have a number of surface trap states where holes can be trapped. Upon the annealing of the surface by UV light, holes cannot be trapped in deep surface trap states and QDs PL is always ‘on’. Thus, UV light exposure can be a cheap and effective way to suppress fluorescence intermittency, where continuous light source is needed.

5. Conclusion

In summary, we found a difference in the PLQY of CdTe/CdS QDs where CdS shell was grown at different TGA/Cd²⁺ ratios. We suggest that the difference in PLQY originates from the different growth mechanism of the CdS shell around CdTe core QDs. At a TGA/Cd²⁺ ratio of 1.3, the CdS shell will form via homogeneous nucleation, which is dependent on diffusion of growth material from the solution onto the QDs surface, where TGA surfactants act as a stopping barrier. However, due to lattice mismatch of core and shell materials, the formed CdS shell experiences coherence strain which will result in dislocation sites and surface defects where carriers can migrate and become trapped [26]. At a TGA/Cd²⁺ ratio of 2, the CdS shell grows epitaxially. In this case, the shell will passivate the core, but will not introduce additional trap states. In addition, fluorescence intermittency was suppressed for HQY CdTe QDs after UV light illumination. This can be explained by annealing of deep surface trap states on the QDs surface by UV light.

Acknowledgments

We extend our acknowledgments to the academic staff of Molecular and Nanoscale Physics Group at the University of Leeds for their valuable insights and for providing us the materials and laboratory facilities.

Disclosure statement

No potential conflict of interest was reported by the authors.

Funding

KC acknowledges the MRC [MR/K015613/1] for financial support.

References

- [1] Rogach AL, Katsikas L, Kornowski A, et al. Synthesis and characterization of thiol-stabilized CdTe nanocrystals. *Ber Bunsenges phys Chem.* 1996;100(11):1772–1778.
- [2] Gaponenko SV. *Optical properties of semiconductor nanocrystals.* Cambridge: Cambridge University Press; 1998.
- [3] Mi W, Tian W, Tian J, et al. Synthesis of CdSe quantum dots in ethanol: a facile way to achieve photoluminescence with high brightness. *Colloid Surf A.* 2013;417(0):179–182.
- [4] Zhang A, Liu N, Cao Y, et al. Photoluminescence stability of colloidal CdTe quantum dots in various buffer solutions. *J Cluster Sci.* 2013;24(2):427–437.
- [5] Talapin DV, Rogach AL, Shevchenko EV, et al. Dynamic distribution of growth rates within the ensembles of colloidal II–VI and III–V semiconductor nanocrystals as a factor governing their photoluminescence efficiency. *J Am Chem Soc.* 2002;124(20):5782–5790.
- [6] Chu VH, Nghiem THL, Le TH, et al. Synthesis and optical properties of water soluble CdSe/CdS quantum dots for biological applications. *Adv Nat Sci: Nanosci Nanotechnol.* 2012;3(2):025017.
- [7] Jiang P, Zhu C-N, Zhang Z-L, et al. Water-soluble Ag₂S quantum dots for near-infrared fluorescence imaging *in vivo*. *Biomaterials.* 2012;33(20):5130–5135.
- [8] Scholes GD. Controlling the optical properties of inorganic nanoparticles. *Adv Funct Mater.* 2008;18(8):1157–1172.
- [9] Talapin DV, Mekis I, Gotzinger S, et al. CdSe/CdS/ZnS and CdSe/ZnSe/ZnS core–shell–shell nanocrystals. *J Phys Chem B.* 2004;108(49):18826–18831.
- [10] Dabbousi BO, Rodriguez-Viejo J, Mikulec FV, et al. (CdSe)ZnS core–shell quantum dots: synthesis and characterization of a size series of highly luminescent nanocrystallites. *J Phys Chem B.* 1997;101(46):9463–9475.
- [11] Resch U, Weller H, Henglein A. Photochemistry and radiation chemistry of colloidal semiconductors. 33. Chemical changes and fluorescence in CdTe and ZnTe. *Langmuir.* 1989;5(4):1015–1020.
- [12] Rogach AL, Franzl T, Klar TA, et al. Aqueous synthesis of thiol-capped CdTe nanocrystals: state-of-the-art. *J Phys Chem C.* 2007;111(40):14628–14637.
- [13] Chen X, Hutchison JL, Dobson PJ, et al. Highly luminescent monodisperse CdSe nanoparticles synthesized in aqueous solution. *J Mater Sci.* 2009;44(1):285–292.
- [14] Gaponik N, Talapin DV, Rogach AL, et al. Thiol-capping of CdTe nanocrystals: an alternative to organometallic synthetic routes. *J Phys Chem B.* 2002;106(29):7177–7185.
- [15] Pons T, Pic E, Lequeux N, et al. Cadmium-free CuInS₂/ZnS quantum dots for sentinel lymph node imaging with reduced toxicity. *ACS Nano.* 2010;4(5):2531–2538.
- [16] Borchert H, Talapin DV, Gaponik N, et al. Relations between the photoluminescence efficiency of CdTe nanocrystals and their surface properties revealed by synchrotron XPS. *J Phys Chem B.* 2003;107(36):9662–9668.
- [17] Crisp MT, Kotov NA. Preparation of nanoparticle coatings on surfaces of complex geometry. *Nano Lett.* 2003;3(2):173–177.
- [18] Zhang H, Wang L, Xiong H, et al. Hydrothermal synthesis for high-quality CdTe nanocrystals. *Adv Mater.* 2003;15(20):1712–1715.
- [19] Guo J, Yang W, Wang C. Systematic study of the photoluminescence dependence of thiol-capped CdTe nanocrystals on the reaction conditions. *J Phys Chem B.* 2005;109(37):17467–17473.
- [20] Li L, Qian H, Ren J. Rapid synthesis of highly luminescent CdTe nanocrystals in the aqueous phase by microwave irradiation with controllable temperature. *Chem Commun.* 2005;36(4):528–530.
- [21] He Y, Lu H-T, Sai L-M, et al. Microwave-assisted growth and characterization of water-dispersed CdTe/CdS core–shell nanocrystals with high photoluminescence. *J Phys Chem B.* 2006;110(27):13370–13374.
- [22] Li L, Qian H, Fang N, et al. Significant enhancement of the quantum yield of CdTe nanocrystals synthesized in aqueous phase by controlling the pH and concentrations of precursor solutions. *J Lumin.* 2006;116(1–2):59–66.

- [23] Shavel A, Gaponik N, Eychmüller A. Factors governing the quality of aqueous CdTe nanocrystals: calculations and experiment. *J Phys Chem B*. 2006;110(39):19280–19284.
- [24] Radtchenko IL, Sukhorukov GB, Gaponik N, et al. Core-shell structures formed by the solvent-controlled precipitation of luminescent CdTe nanocrystals on latex spheres. *Adv Mater*. 2001;13(22):1684–1687.
- [25] Jasprit S. *Physics of semiconductors and their heterostructures*. New York (NY): McGraw-Hill; 1993.
- [26] Chen X, Lou Y, Samia AC, et al. Coherency strain effects on the optical response of core/shell heteronanostructures. *Nano Lett*. 2003;3(6):799–803.
- [27] Bao H, Gong Y, Li Z, et al. Enhancement effect of illumination on the photoluminescence of water-soluble CdTe nanocrystals: toward highly fluorescent CdTe/CdS core–shell structure. *Chem Mater*. 2004;16(20):3853–3859.
- [28] Aldana J, Wang YA, Peng X. Photochemical instability of CdSe nanocrystals coated by hydrophilic thiols. *J Am Chem Soc*. 2001;123(36):8844–8850.
- [29] Bin Xu BC, Liu M, Fan H. Ultraviolet radiation synthesis of water dispersed CdTe/CdS/ZnS core?shell?shell quantum dots with high fluorescence strength and biocompatibility. *Nanotechnology*. 2014;24(20):205601.
- [30] Li C, Murase N. Surfactant-dependent photoluminescence of CdTe nanocrystals in aqueous solution. *Chem Lett*. 2005;34(1):92–93.
- [31] Wang C, Zhang H, Xu S, et al. Sodium-citrate-assisted synthesis of aqueous CdTe nanocrystals: giving new insight into the effect of ligand shell. *J Phys Chem C*. 2009;113(3):827–833.
- [32] Kubin RF, Fletcher AN. Fluorescence quantum yields of some rhodamine dyes. *J Lumin*. 1982;27(4):455–462.
- [33] Crosby GA, Demas JN. Measurement of photoluminescence quantum yields. Review. *J Phys Chem*. 1971;75(8):991–1024.
- [34] Gerion D, Pinaud F, Williams SC, et al. Synthesis and properties of biocompatible water-soluble silica-coated CdSe/ZnS semiconductor quantum dots. *J Phys Chem B*. 2001;105(37):8861–8871.
- [35] Gluzman A, Lifshitz E, Hoppe K, et al. Optically detected magnetic resonance of thiol-capped CdTe nanocrystals. *Isr J Chem*. 2001;41(1):39–44.
- [36] Talapin DV, Rogach AL, Haase M, et al. Evolution of an ensemble of nanoparticles in a colloidal solution: theoretical study. *J Phys Chem B*. 2001;105(49):12278–12285.
- [37] Klimov VI, Mikhailovsky AA, McBranch DW, et al. Quantization of multiparticle Auger rates in semiconductor quantum dots. *Science*. 2000;287(5455):1011–1013.
- [38] García-Santamaría F, Brovelli S, Viswanatha R, et al. Breakdown of volume scaling in Auger recombination in CdSe/CdS heteronanostructures: the role of the core–shell interface. *Nano Lett*. 2011;11(2):687–693.
- [39] Park Y-S, Bae WK, Padilha LA, et al. Effect of the core/shell interface on Auger recombination evaluated by single-quantum-dot spectroscopy. *Nano Lett*. 2014;14(2):396–402.
- [40] Cragg GE, Efras AL. Suppression of Auger processes in confined structures. *Nano Lett*. 2009;10(1):313–317.
- [41] Chen Y, Vela J, Htoon H, et al. “Giant” multishell CdSe nanocrystal quantum dots with suppressed blinking. *J Am Chem Soc*. 2008;130(15):5026–5027.
- [42] Mahler B, Spinicelli P, Buil S, et al. Towards non-blinking colloidal quantum dots. *Nat Mater*. 2008;7(8):659–664.
- [43] Frantsuzov PA, Marcus RA. Explanation of quantum dot blinking without the long-lived trap hypothesis. *Phys Rev B*. 2005;72(15):155321.